• Basic Research •

Multi-omics Mendelian randomization analysis identifies SPATA20 as a cross-omic target in primary open angle glaucoma

Zhi-Kun Ouyang[1], *Ling Ge*[1], *Shi-Tong Yu*[2], *Jing-Yi Luo*[3]

[1]Shanghai Eye Diseases Prevention & Treatment Center/ Shanghai Eye Hospital, School of Medicine, Tongji University, National Clinical Research Center for Eye Diseases, Shanghai Engineering Research Center of Precise Diagnosis and Treatment of Eye Diseases, Shanghai 200041, China
[2]Department of General Surgery, Nanfang Hospital, Southern Medical University, Guangzhou 510515, Guangdong Province, China
[3]Department of Ophthalmology, The Third Affiliated Hospital of Sun Yat-sen University, Guangzhou 510630, Guangdong Province, China
Correspondence to: Jing-Yi Luo. Department of Ophthalmology, The Third Affiliated Hospital of Sun Yat-sen University, Guangzhou 510630, Guangdong Province, China. camel043@126.com; Shi-Tong Yu. Department of General Surgery, Nanfang Hospital, Southern Medical University, Guangzhou 510515, Guangdong Province, China. yusht@smu.edu.cn
Received: 2026-02-07 Accepted: 2026-04-10

Abstract

● **AIM:** To investigate the mitochondrial dysfunction-related genes and their regulatory mechanisms involved in primary open angle glaucoma (POAG), which is characterized by retinal ganglion cell loss.

● **METHODS:** Multi-omic summary-data-based Mendelian randomization (SMR) integrating methylation quantitative trait loci (mQTL), expression quantitative trait loci (eQTL), and protein quantitative trait loci (pQTL) were performed for mitochondrial genes with genome-wide association studies (GWAS) of POAG and related traits [intraocular pressure (IOP), macular retinal nerve fiber layer thickness (mRNFL), and macular ganglion cell-inner plexiform layer thickness (mGCIPL)]. Bayesian colocalization was used to support shared causal variants and to define evidence tiers across omics. SPATA20 expression was assessed in a mouse glaucoma model by immunofluorescence and Western blot.

● **RESULTS:** SMR identified 64 mitochondrial genes associated with at least one outcome, including *ALDH18A1* for POAG and *MRPL55* for mRNFL. eQTL analysis revealed 212 associations, prioritizing *MRPL20*, *SLC25A26*, *ALAS1*, and *GLYCTK* for POAG, *ACAD10* for IOP, *ALDH6A1*, *GRPEL2*, and *YARS2* for mRNFL, and *ALDH6A1*, *TIMM21*, *TIMM29*, *LARS2*, and *METAP1D* for mGCIPL. The pQTL layer implicated 21 proteins, including BOLA1 for POAG. Cross-omic synthesis supported 18 genes by ≥2 omics layers. SPATA20 was supported by all three layers, showed a consistent negative association with mRNFL, and in mice was transiently upregulated in retina, with expression in the ganglion cell layer.

● **CONCLUSION:** Multi-omic SMR with colocalization highlights mitochondrial genes for POAG and related traits and nominates SPATA20 as a leading cross-omics signal for mRNFL.

● **KEYWORDS:** primary open angle glaucoma; glaucoma-related traits; Mendelian randomization; mitochondrion; methylation; gene expression; SPATA20

DOI:10.18240/ijo.2026.08.03

Citation: Ouyang ZK, Ge L, Yu ST, Luo JY. Multi-omics Mendelian randomization analysis identifies SPATA20 as a cross-omic target in primary open angle glaucoma. *Int J Ophthalmol* 2026;19(8):1451-1460

INTRODUCTION

Glaucoma is a leading irreversible blindness characterized by progressive degeneration of the optic nerve and retinal ganglion cells (RGCs)[1]. Based on the anatomy of anterior chamber angle, primary glaucoma can be categorized into primary open angle glaucoma (POAG) and primary angle-closure glaucoma, with POAG being the predominant type. Intraocular pressure (IOP) is the major risk factor for glaucoma, mainly linked to the impaired trabecular meshwork cell (TMC) function. In recent years, numerous studies have highlighted the pivotal role of mitochondria in the pathogenesis of glaucoma. Mitochondrial dysfunction may lead to intracellular energy deficits and oxidative stress, which can initiate apoptosis in both TMCs and RGCs[2]. Genome-wide association studies (GWAS) and experimental research

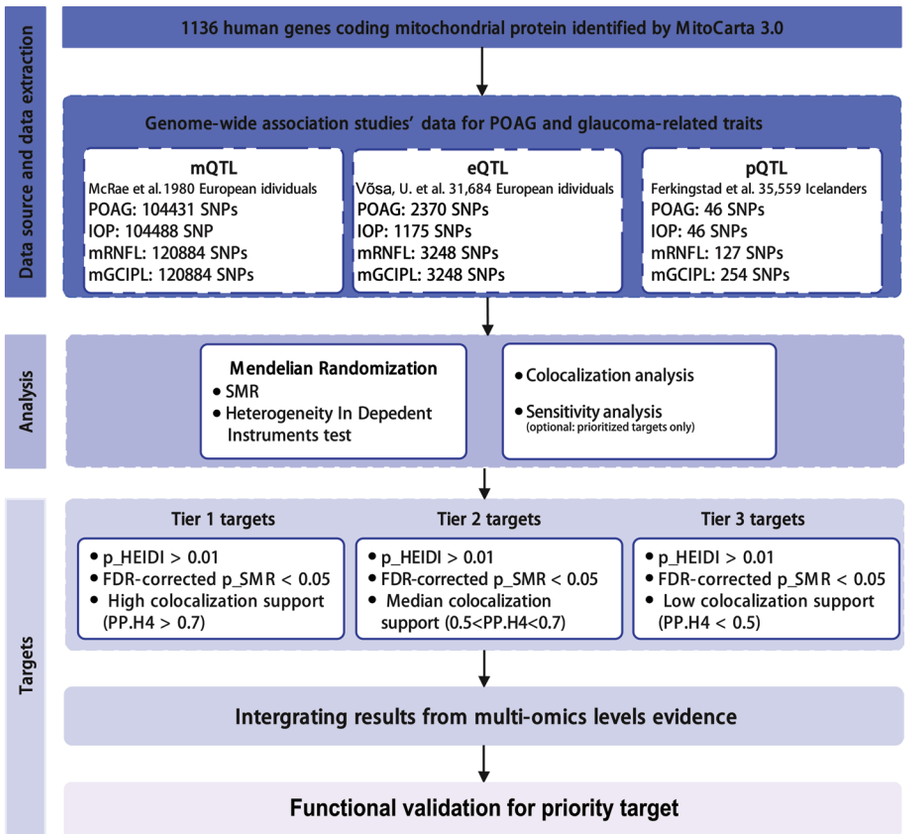

Figure 1 Study design of study SMR: Summary-based Mendelian randomization; QTL: Quantitative trait loci; POAG: Primary open angle glaucoma; eQTL: Expression quantitative trait loci; pQTL: Protein quantitative trait loci; mQTL: Methylation quantitative trait loci; HEIDI: Heterogeneity in dependent instrument; IOP: Intraocular pressure; mRNFL: Macular retinal nerve fiber layer; mGCIPL: Macular ganglion cell-inner plexiform layer; SNP: Single nucleotide polymorphisms; PP.H4: Posterior probability for hypothesis 4; FDR: False discovery rate.

have identified multiple POAG susceptibility genes associated with mitochondria, including *MYOC*, which is linked to TMCs dysfunction[3], and *OPA1*, *OPTN*, and *CYP1B1*, which are implicated in the pathogenesis of RGCs[4-6]. Although the crucial role of the mitochondrion in POAG is now recognized, the specific mitochondrial-related genes and their regulatory mechanism in POAG remain elusive.

Gene methylation quantitative trait loci (mQTLs), expression quantitative trait loci (eQTLs), and protein quantitative trait loci (pQTLs) encapsulate integrative omics data, offering valuable insights into the biological mechanisms underlying diseases at the levels of DNA methylation, gene expression and protein abundance levels[7]. Mendelian randomization (MR) analysis harnesses genetic information as instrumental variables (IVs) to enhance causal inference between exposures and outcomes. Unlike traditional observational studies, MR is less susceptible to the confounding factors and reverse causation, as genetic variants are randomly assigned and remain constant from conception, preceding the onset of the disease[8]. By incorporating single nucleotide polymorphisms (SNPs) linked to diseases based on mQTL, eQTL, and pQTL datasets, we employed summary-data-based MR (SMR) to investigate the causal associations of mitochondrial gene methylation, expression, and protein abundance with POAG risk. Additionally, we explored the associations between mitochondrial-related genes and glaucoma-related traits, encompassing IOP, macular retinal nerve fiber layer (mRNFL) thickness, and macular ganglion cell-inner plexiform layer (mGCIPL) thickness.

MATERIALS AND METHODS

Ethical Approval This study used publicly available, summary-level GWAS datasets and did not involve access to individual-level data. Therefore, ethics approval and informed consent for this study were not required. Ethics approval and participant consent were obtained in the original GWAS studies, as described in the corresponding publications.

Figure 1 illustrates the overall design of this study. The current SMR analysis relies on publicly available datasets, namely the International Glaucoma Genetics Consortium[9] and the UK Biobank[10]. In this study, IVs for mitochondrial genes were extracted at the methylation, gene expression, and protein abundance levels. As the main analysis strategies, SMR analyses were conducted independently for POAG and glaucoma-related traits at each of these biological levels. Colocalization analyses were applied to strengthen the causal inferences.

Data Sources for Mitochondrial-Related Genes, mQTL, eQTL, and pQTL Datasets Integration of multi-omics data provides deeper insight into the molecular networks underlying mitochondrial dysfunction. A total of 1136 human mitochondrial-related genes were identified based on the updated inventory from MitoCarta3.0[11] (https://www.broadinstitute.org/files/shared/metabolism/mitocarta/human.mitocarta3.0.html). SNP-CpG associations in blood were obtained from mQTL data by McRae *et al*[12] in European ancestry individuals (n=1980). The cis-mQTL for genetic variants closely related to mitochondrial-related genes was extracted. The aggregated statistical data of blood eQTL were obtained from the eQTLGen Consortium[13], which included 31 684 individuals (https://www.eQTLGen.com). We included cis-eQTLs located within 1000 kb upstream of the transcription start site or 1000 kb downstream of the transcription end site of the target genes. The statistics of 28 191 genetic associations with 4907 circulating protein levels were obtained from a pQTL study that included 35 559 Icelanders[14].

GWAS Data of POAG and Glaucoma-Related Traits The largest GWAS data summary statistics of open angle glaucoma, namely, POAG were extracted from International Glaucoma Genetics Consortium, comprising 14 822 926 SNPs from a cohort of 16 677 participants and 199 580 controls of European descent. The definition of POAG was based on the International Classification of Diseases diagnostic codes (ICD-9/ICD-10 revisions). Summary statistics for glaucoma-related traits were also extracted from GWAS studies of European individuals, including IOP[15] (11 458 861 SNPs), mRNFL[16] (9 121 075 SNPs), and mGCIPL[16] (9 121 075 SNPs).

SMR Analysis The SMR analysis was the primary analysis for this study, which was employed to test for potential causal associations between mitochondrial-related molecular traits (mQTL, eQTL, and pQTL) and outcomes of glaucoma with its corresponding traits. This method utilizes the top cis-acting genetic variant associated with a molecular trait as an instrumental variable.

SNPs significantly associated with exposure factors were used as IVs, which were screened according to the following criteria: 1) SNPs strongly associated with the exposure (P<5×10^{-8}) were selected as candidate IVs; 2) SNPs in high linkage disequilibrium with the top SNP (R^2>0.9) were pruned, and only those with R^2≤0.9 were retained for analysis; 3) To ensure independence among IVs, clumping against the 1000 Genomes European population reference (r^2<0.001, 10 000-kb window), retaining the lead SNP per region.

To distinguish whether a significant SMR signal was driven by a single causal variant versus multiple correlated variants due to linkage disequilibrium, the Heterogeneity in Dependent Instruments (HEIDI) test was applied. P_{HEIDI}>0.01 were indicates no evidence of heterogeneity, consistent with a single shared variant rather than distinct linked variants. Associations meeting the dual thresholds of P_{SMR}<0.05 [false discovery rate (FDR) corrected using the Benjamini-Hochberg method) and P_{HEIDI}>0.01 were taken forward for interpretation.

Sensitivity analyses were conducted as a supplementary analysis, which was only when ≥3 independent cis SNPs are available. These analyses were not used to define primary findings.

Colocalization Analysis We employed Bayesian colocalization analyses to detect shared causal variants between identified mitochondrial-related associations and POAG and glaucoma-related traits using the *R* package "coloc"[17]. All associations meeting the criteria of FDR-adjusted P_{SMR}<0.05 and P_{HEIDI}>0.01 were then assessed with 5 different hypotheses (H0–H4) by generating different posterior probabilities (PP). H0 suggests the absence of any association with both exposure and outcome, whereas H4 suggests a shared causal variant associated with exposure and outcome. A posterior probability for hypothesis 4 (PP.H4)>0.70 was considered significant evidence for colocalization.

Integrating Results from Multi-Omics Level of Evidence To comprehensively assess how mitochondrial-related genes associate with glaucoma across multiple biological levels, we integrated evidence from three distinct regulatory tiers. In this study, PP.H4>0.7 is considered strong evidence for colocalization (Tier 1 targets). Medium colocalization was defined as 0.5<PP.H4<0.7 (Tier 2 targets). For those associations with P_{SMR}<0.05 and P_{HEIDI}>0.01 but PP.H4<0.5 (Tier 3 targets), the results can still offer insights into understanding the relationship between mitochondrial genes and glaucoma.

Glaucoma Mouse Model The optic nerve crush (ONC) model was used as the glaucomatous optic neuropathy paradigm following an established protocol[18]. Under general and local anesthesia, a superior-lateral conjunctival incision was made, orbital muscles were retracted to expose the optic nerve, and the nerve was crushed approximately 1 mm posterior to the globe using self-clamping forceps for 5s. Sham-operated controls underwent the same exposure procedure without nerve crush. Eyes were harvested at 1, 3, 7, and 10d post-procedure. This study was approved by the Ethics Committee of Shanghai Eye Disease Prevention and Treatment Center (TBJ04625279).

Western Blot Analysis Retinal proteins were extracted and quantified, separated by 10% sodium dodecyl sulfate-polyacrylamide gel electrophoresis (SDS-PAGE), transferred to polyvinylidene difluoride (PVDF) membranes, and blocked in 5% skim milk. Membranes were incubated overnight at 4°C with rabbit anti-SPATA20 (1:1000; 18373-1-AP, Proteintech),

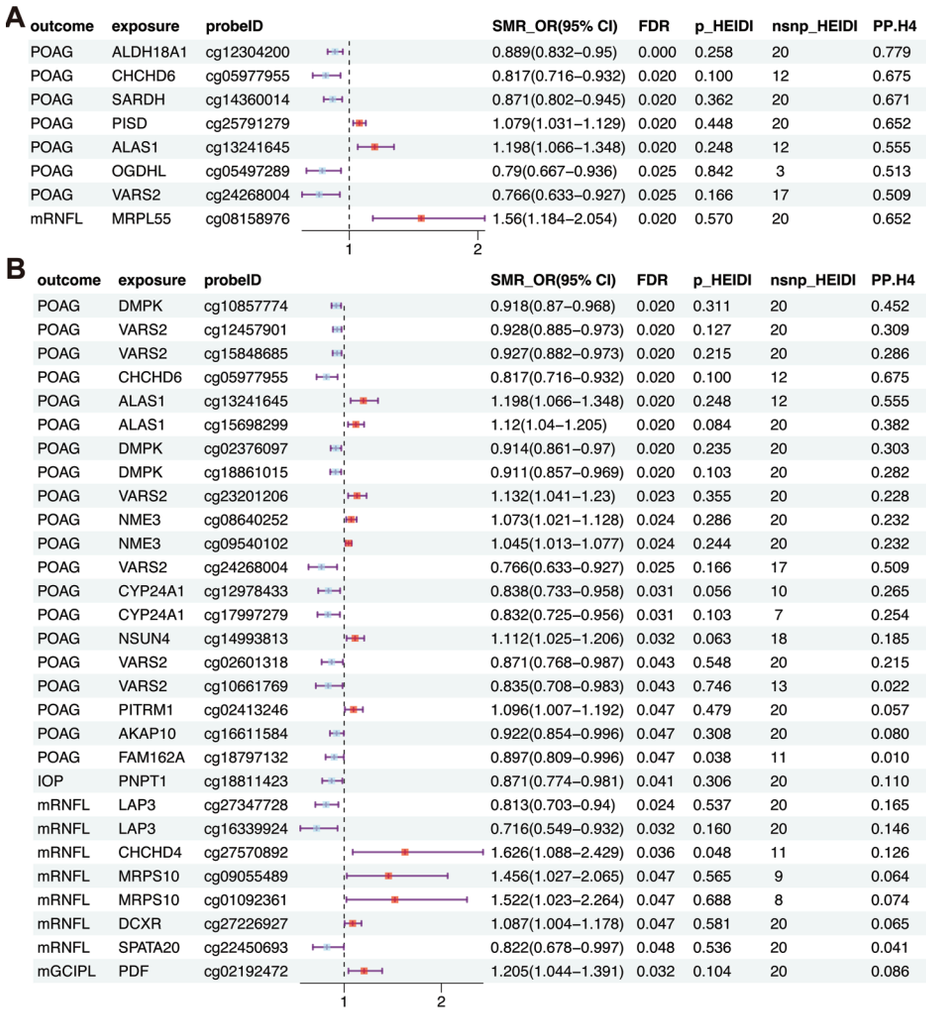

A

outcome	exposure	probeID	SMR_OR(95% CI)	FDR	p_HEIDI	nsnp_HEIDI	PP.H4
POAG	ALDH18A1	cg12304200	0.889(0.832–0.95)	0.000	0.258	20	0.779
POAG	CHCHD6	cg05977955	0.817(0.716–0.932)	0.020	0.100	12	0.675
POAG	SARDH	cg14360014	0.871(0.802–0.945)	0.020	0.362	20	0.671
POAG	PISD	cg25791279	1.079(1.031–1.129)	0.020	0.448	20	0.652
POAG	ALAS1	cg13241645	1.198(1.066–1.348)	0.020	0.248	12	0.555
POAG	OGDHL	cg05497289	0.79(0.667–0.936)	0.025	0.842	3	0.513
POAG	VARS2	cg24268004	0.766(0.633–0.927)	0.025	0.166	17	0.509
mRNFL	MRPL55	cg08158976	1.56(1.184–2.054)	0.020	0.570	20	0.652

B

outcome	exposure	probeID	SMR_OR(95% CI)	FDR	p_HEIDI	nsnp_HEIDI	PP.H4
POAG	DMPK	cg10857774	0.918(0.87–0.968)	0.020	0.311	20	0.452
POAG	VARS2	cg12457901	0.928(0.885–0.973)	0.020	0.127	20	0.309
POAG	VARS2	cg15848685	0.927(0.882–0.973)	0.020	0.215	20	0.286
POAG	CHCHD6	cg05977955	0.817(0.716–0.932)	0.020	0.100	12	0.675
POAG	ALAS1	cg13241645	1.198(1.066–1.348)	0.020	0.248	12	0.555
POAG	ALAS1	cg15698299	1.12(1.04–1.205)	0.020	0.084	20	0.382
POAG	DMPK	cg02376097	0.914(0.861–0.97)	0.020	0.235	20	0.303
POAG	DMPK	cg18861015	0.911(0.857–0.969)	0.020	0.103	20	0.282
POAG	VARS2	cg23201206	1.132(1.041–1.23)	0.023	0.355	20	0.228
POAG	NME3	cg08640252	1.073(1.021–1.128)	0.024	0.286	20	0.232
POAG	NME3	cg09540102	1.045(1.013–1.077)	0.024	0.244	20	0.232
POAG	VARS2	cg24268004	0.766(0.633–0.927)	0.025	0.166	17	0.509
POAG	CYP24A1	cg12978433	0.838(0.733–0.958)	0.031	0.056	10	0.265
POAG	CYP24A1	cg17997279	0.832(0.725–0.956)	0.031	0.103	7	0.254
POAG	NSUN4	cg14993813	1.112(1.025–1.206)	0.032	0.063	18	0.185
POAG	VARS2	cg02601318	0.871(0.768–0.987)	0.043	0.548	20	0.215
POAG	VARS2	cg10661769	0.835(0.708–0.983)	0.043	0.746	13	0.022
POAG	PITRM1	cg02413246	1.096(1.007–1.192)	0.047	0.479	20	0.057
POAG	AKAP10	cg16611584	0.922(0.854–0.996)	0.047	0.308	20	0.080
POAG	FAM162A	cg18797132	0.897(0.809–0.996)	0.047	0.038	11	0.010
IOP	PNPT1	cg18811423	0.871(0.774–0.981)	0.041	0.306	20	0.110
mRNFL	LAP3	cg27347728	0.813(0.703–0.94)	0.024	0.537	20	0.165
mRNFL	LAP3	cg16339924	0.716(0.549–0.932)	0.032	0.160	20	0.146
mRNFL	CHCHD4	cg27570892	1.626(1.088–2.429)	0.036	0.048	11	0.126
mRNFL	MRPS10	cg09055489	1.456(1.027–2.065)	0.047	0.565	9	0.064
mRNFL	MRPS10	cg01092361	1.522(1.023–2.264)	0.047	0.688	8	0.074
mRNFL	DCXR	cg27226927	1.087(1.004–1.178)	0.047	0.581	20	0.065
mRNFL	SPATA20	cg22450693	0.822(0.678–0.997)	0.048	0.536	20	0.041
mGCIPL	PDF	cg02192472	1.205(1.044–1.391)	0.032	0.104	20	0.086

Figure 2 Associations of genetically predicted mitochondrial gene methylation with POAG and its endophenotypes A: Associations identified as Tier 1 or Tier 2 targets; B: Associations significant in at two or three omics levels. SMR: Summary-data-based Mendelian randomization; OR: Odds ratio; CI: Confidence interval; nsnp: Number of single nucleotide polymorphisms; HEIDI: Heterogeneity in dependent instrument; PP.H4: Posterior probability for hypothesis 4; FDR: False discovery rate; POAG: Primary open angle glaucoma; IOP: Intraocular pressure; mRNFL: Macular retinal nerve fiber layer; mGCIPL: Macular ganglion cell-inner plexiform layer.

followed by horseradish-peroxidase (HRP)-conjugated goat anti-rabbit immunoglobulin G (IgG) secondary antibody (1:2000). Bands were visualized by chemiluminescence and quantified using ImageJ (LOCI, University of Wisconsin, USA).

Tissue Processing and Immunostaining Mice were euthanized by anesthetic overdose and perfused with phosphate buffered saline (PBS) followed by 4% paraformaldehyde. Eyes were post-fixed, cryoprotected in graded sucrose (10%, 20%, 30%), embedded in optimal cutting temperature compound, and sectioned at 13 μm. Sections were incubated with rabbit anti-SPATA20 (1:200) overnight at 4°C, followed by Alexa Fluor-conjugated secondary antibodies (1:500) and 4',6-diamidino-2-phenylindole (DAPI) counterstaining (1:2000). Fluorescence images were captured at a distance of 300 μm from the optic nerve head, and immunopositivity in the whole retina and ganglion cell layer (GCL) was quantified by thresholding under uniform imaging conditions as previously described[18].

RESULTS

Mitochondrial Gene Methylation Analysis We first examined the association between mitochondrial DNA methylation and glaucoma risk. Across 415 methylation sites, 82 were significant (P_{SMR}<0.05 and P_{HEIDI}>0.01), mapping to 64 genes. For POAG, *ALDH18A1* was the unique Tier 1 target: decreased methylation at cg12304200 was linked to reduced risk. Six Tier 2 loci were identified (*CHCHD6, SARDH*, *PISD*, *ALAS1*, *OGDHL*, and *VARS2*). For mRNFL, *MRPL55* (cg08158976) was Tier 2, whereas mGCIPL and IOP showed only Tier 3 signals (Figure 2A). Figure 2B highlights 29 CpG sites across 16 genes significant in at least two omics levels, including *SPATA20* (cg22450693) for mRNFL.

Mitochondrial Gene Expression Analysis We next assessed gene expression using eQTL data. Among 637 genes with 10 042 SNPs, 212 showed significant associations. Genetically predicted increased expression of *SLC25A26*,

A

outcome	exposure	SMR_OR(95% CI)	p_SMR	p_HEIDI	nsnp_HEIDI	PP.H4
POAG	MRPL20	0.774(0.675–0.887)	0.000	0.239	20	0.871
POAG	SLC25A26	1.427(1.171–1.738)	0.000	0.079	20	0.832
POAG	ISCA2	1.09(1.04–1.142)	0.000	0.192	20	0.662
POAG	GLYCTK	1.114(1.044–1.189)	0.001	0.178	20	0.764
POAG	ALAS1	0.624(0.472–0.824)	0.001	0.143	20	0.717
POAG	ATPSCKMT	0.625(0.468–0.835)	0.001	0.483	20	0.683
POAG	COX17	0.744(0.617–0.896)	0.002	0.245	16	0.653
IOP	ACAD10	3.761(1.819–7.777)	0.000	0.221	16	0.976
mRNFL	ALDH6A1	171.085(36.989–791.323)	0.000	0.109	20	1.000
mRNFL	YARS2	0.193(0.072–0.517)	0.001	0.989	20	0.893
mRNFL	GRPEL2	0.315(0.163–0.607)	0.001	0.104	20	0.752
mRNFL	CHCHD4	0.204(0.068–0.609)	0.004	0.016	20	0.512
mGCIPL	ALDH6A1	118.456(21.419–655.097)	0.000	0.345	20	1.000
mGCIPL	TIMM29	0.182(0.089–0.374)	0.000	0.514	20	0.998
mGCIPL	LARS2	0.475(0.342–0.659)	0.000	0.012	20	0.991
mGCIPL	METAP1D	0.173(0.073–0.411)	0.000	0.267	20	0.972
mGCIPL	TIMM21	2.447(1.479–4.047)	0.000	0.423	20	0.750
mGCIPL	GTPBP3	0.365(0.197–0.674)	0.001	0.014	20	0.550

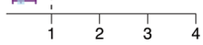

B

outcome	exposure	SMR_OR(95% CI)	p_SMR	p_HEIDI	nsnp_HEIDI	PP.H4
POAG	CHCHD6	2.333(1.483–3.669)	0.000	0.523	20	0.208
POAG	ALAS1	0.624(0.472–0.824)	0.001	0.143	20	0.717
POAG	CYP24A1	1.376(1.116–1.695)	0.003	0.209	20	0.444
POAG	DMPK	0.875(0.799–0.957)	0.004	0.148	20	0.288
POAG	AKAP10	1.06(1.017–1.105)	0.005	0.170	20	0.010
POAG	NSUN4	0.947(0.908–0.987)	0.010	0.098	20	0.009
POAG	NME3	0.825(0.709–0.961)	0.013	0.435	20	0.066
POAG	VARS2	1.147(1.028–1.28)	0.014	0.095	20	0.469
POAG	FAM162A	0.734(0.575–0.939)	0.014	0.764	20	0.119
POAG	PITRM1	1.054(1.003–1.108)	0.036	0.517	20	0.008
IOP	PNPT1	1.433(1.025–2.005)	0.036	0.117	20	0.110
mRNFL	CHCHD4	0.204(0.068–0.609)	0.004	0.016	20	0.512
mRNFL	LAP3	1.136(1.035–1.247)	0.008	0.350	20	0.030
mRNFL	MRPS10	0.618(0.402–0.951)	0.028	0.164	20	0.062
mRNFL	DCXR	0.887(0.79–0.995)	0.040	0.899	20	0.209
mRNFL	SPATA20	0.927(0.862–0.998)	0.043	0.320	20	0.008
mGCIPL	PDF	0.499(0.293–0.849)	0.010	0.077	20	0.142
mGCIPL	GSTZ1	1.406(1.022–1.935)	0.036	0.054	20	0.050

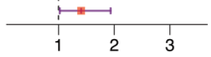

Figure 3 Associations of genetically predicted mitochondrial gene expression with POAG and its endophenotypes A: Associations identified as Tier 1 or Tier 2 targets; B: Associations significant in at two or three omics levels. SMR: Summary-data-based Mendelian randomization; OR: Odds ratio; CI: Confidence interval; nsnp: Number of single nucleotide polymorphisms; HEIDI: Heterogeneity in dependent instrument; PP.H4: Posterior probability for hypothesis 4; POAG: Primary open angle glaucoma; IOP: Intraocular pressure; mRNFL: Macular retinal nerve fiber layer; mGCIPL: Macular ganglion cell-inner plexiform layer.

GLYCTK, and *ISCA2* elevated POAG risk, whereas *MRPL20*, *ALAS1*, *ATPSCKMT*, and *COX17* were protective. *SLC25A26*, *GLYCTK*, *MRPL20*, and *ALAS1* were Tier 1 for POAG, with others as Tier 2. For IOP, increased expression of *ACAD10* was a positive Tier 1 association. Regarding Tier 1 targets for mRNFL thickness, *ALDH6A1* expression was positively linked, while *YARS2* and *GRPEL2* were inversely linked. *CHCHD4* was also inversely associated with mRNFL as a Tier 2 target. For Tier 1 targets for mGCIPL, *ALDH6A1*, and *TIMM21* increased thickness, whereas *TIMM29*, *LARS2*, and *METAP1D* decreased it. *GTPBP3*, a Tier 2 target, was also inversely associated with mGCIPL (Figure 3A). Multi-omics overlap highlighted SPATA20 as a negative mRNFL association (Figure 3B). Sensitivity analyses of the significant associations revealed that 143 had no heterogeneity, whereas 21 did; horizontal pleiotropy was absent in 71 associations.

Mitochondrial Protein Analysis Plasma protein QTL analysis implicated 21 in causal associations with POAG and its related traits. For POAG, higher genetically predicted BOLA1 levels increased risk, qualifying as a Tier 2 target. In addition, 2 proteins were Tier 3 for POAG, 1 for mRNFL, and 2 for mGCIPL. Twelve mitochondrial proteins were significant across at least two omics (Figure 4). Sensitivity analyses indicated 9 proteins had no heterogeneity and 8 showed no horizontal pleiotropy.

Integrating Evidence from Multi-Omics Levels After the integration of evidence from multi-omics, we defined a total of 18 key genes overlapping between any two of the mQTL, eQTL, and pQTL for the same outcome (Figure 5). Specifically, 10 genes (*AKAP10*, *ALAS1*, *CHCHD6*, *CYP24A1*, *DMPK*, *FAM162A*, *NME3*, *NSUN4*, *PITRM1*, and *VARS2*) were identified as key genes for POAG; *PNPT1* for IOP; 5

outcome	exposure	SMR_OR(95% CI)	p_SMR	p_HEIDI	nsnp_HEIDI	PP.H4
POAG	BOLA1	1.071(1.018–1.126)	0.008	0.110	20	0.665
mRNFL	SPATA20	0.795(0.632–0.999)	0.049	0.341	20	0.036
mGCIPL	GSTZ1	1.093(1.002–1.192)	0.045	0.040	20	0.011

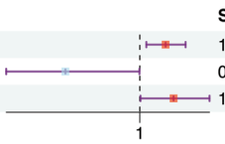

Figure 4 Associations of genetically predicted mitochondrial gene encoded protein with POAG and its endophenotypes Associations identified as Tier 1 or Tier 2 targets. SMR: Summary-data-based Mendelian randomization; OR: Odds ratio; CI: Confidence interval; nsnp: Number of single nucleotide polymorphisms; HEIDI: Heterogeneity in dependent instrument; PP.H4: Posterior probability for hypothesis 4; POAG: Primary open angle glaucoma; mRNFL: Macular retinal nerve fiber layer; mGCIPL: Macular ganglion cell-inner plexiform layer.

Catalogue	Exposure	mQTL			eQTL		pQTL	
		probeID	SMR_OR (95%CI)	*P*	SMR_OR (95%CI)	*P*	SMR_OR (95%CI)	*P*
IOP	PNPT1	cg18811423	0.871(0.774-0.981)	0.023	1.433(1.025-2.005)	0.036		
POAG	AKAP10	cg16611584	0.922(0.854-0.996)	0.0469	1.06(1.017-1.105)	0.0222		
	ALAS1	cg13241645	1.198(1.066-1.348)	0.0196	0.624(0.472-0.824)	0.0089		
	ALAS1	cg15698299	1.12(1.04-1.205)	0.0196	0.624(0.472-0.825)	0.0089		
	CHCHD6	cg05977955	0.817(0.716-0.932)	0.0196	2.333(1.483-3.669)	0		
	CYP24A1	cg12978433	0.838(0.733-0.958)	0.0315	1.376(1.116-1.695)	0.0191		
	CYP24A1	cg17997279	0.832(0.725-0.956)	0.0315	1.376(1.116-1.696)	0.0191		
	DMPK	cg10857774	0.918(0.87-0.968)	0.0196	0.875(0.799-0.957)	0.0204		
	DMPK	cg02376097	0.914(0.861-0.97)	0.0196	0.875(0.799-0.957)	0.0204		
	DMPK	cg18861015	0.911(0.857-0.969)	0.0196	0.875(0.799-0.957)	0.0204		
	FAM162A	cg18797132	0.897(0.809-0.996)	0.0469	0.734(0.575-0.939)	0.0325		
	NME3	cg08640252	1.073(1.021-1.128)	0.0236	0.825(0.709-0.961)	0.0312		
	NME3	cg09540102	1.045(1.013-1.077)	0.0236	0.825(0.709-0.962)	0.0312		
	NSUN4	cg14993813	1.112(1.025-1.206)	0.0319	0.947(0.908-0.987)	0.0304		
	PITRM1	cg02413246	1.096(1.007-1.192)	0.0466	1.054(1.003-1.108)	0.0453		
	VARS2	cg24268004	0.766(0.633-0.927)	0.0255	1.147(1.028-1.28)	0.0325		
	VARS2	cg12457901	0.928(0.885-0.973)	0.0196	1.147(1.028-1.28)	0.0325		
	VARS2	cg15848685	0.927(0.882-0.973)	0.0196	1.147(1.028-1.28)	0.0325		
	VARS2	cg23201206	1.132(1.041-1.23)	0.0227	1.147(1.028-1.28)	0.0325		
	VARS2	cg02601318	0.871(0.768-0.987)	0.0432	1.147(1.028-1.28)	0.0325		
	VARS2	cg10661769	0.835(0.708-0.983)	0.0432	1.147(1.028-1.28)	0.0325		
mRNFL	CHCHD4	cg27570892	1.626(1.088-2.429)	0.0364	0.204(0.068-0.609)	0.0204		
	DCXR	cg27226927	1.087(1.004-1.178)	0.0469	0.887(0.79-0.995)	0.0469		
	LAP3	cg27347728	0.813(0.703-0.94)	0.0236	1.136(1.035-1.247)	0.0291		
	LAP3	cg16339924	0.716(0.549-0.932)	0.0325				
	MRPS10	cg01092361	1.522(1.023-2.264)	0.0469	0.618(0.402-0.951)	0.0436		
	MRPS10	cg09055489	1.456(1.027-2.065)	0.0469				
	SPATA20	**cg22450693**	**0.822(0.678-0.997)**	**0.0477**	**0.927(0.862-0.998)**	**0.0479**	**0.795(0.632-0.999)**	**0.049**
mGCIPL	PDF	cg02192472	1.205(1.044-1.391)	0.0319	0.499(0.293-0.849)	0.0304		
	GSTZ1				1.406(1.022-1.935)	0.0453	1.093(1.002-1.192)	0.049

Figure 5 Integrating evidence from multi-omics levels All *P* are FDR adjusted values. SMR: Summary-based Mendelian randomization; POAG: Primary open angle glaucoma; eQTL: Expression quantitative trait loci; pQTL: Protein quantitative trait loci; mQTL: Methylation quantitative trait loci; IOP: Intraocular pressure; mRNFL: Macular retinal nerve fiber layer; mGCIPL: Macular ganglion cell-inner plexiform layer; OR: Odds ratio; CI: Confidence interval; FDR: False discovery rate.

genes (*CHCHD4*, *DCXR*, *LAP3*, *MRPS10*, and *SPATA20*) for mRNFL thickness; and 2 genes (*PDF* and *GSTZ1*) for mGCIPL thickness. Across these 18 genes, methylation- and expression-based directions were concordant for only four gene–trait pairs (*DMPK*, *FAM162A*, and *PITRM1* with POAG and for *SPATA20* with mRNFL), while most others were directionally discordant. Nevertheless, *SPATA20* was directionally consistent SMR estimates across the mQTL probe, eQTL, and pQTL instruments for the mRNFL trait, making it the highest-confidence cross-omics target.

Expression Pattern of SPATA20 in Glaucomatous Retina To better explore and understand the pathogenic role of SPATA20 in glaucoma, we profiled its expression pattern in the ONC mouse model. Following ONC, retinal SPATA20 expression increased remarkably, peaking at day 3, and declining thereafter. Immunostaining localized the protein of SPATA20 to the GCL and inner nuclear layer in the glaucomatous condition, with quantitative analyses showing significant upregulation in both layers within the first three days and maximal signal on day 3 (Figure 6). These findings aligned with our SMR analysis, showing a negative correlation between SPATA20 expression and mRNFL thickness. Collectively, the data implicate SPATA20 as an early marker of glaucomatous optic neuropathy change.

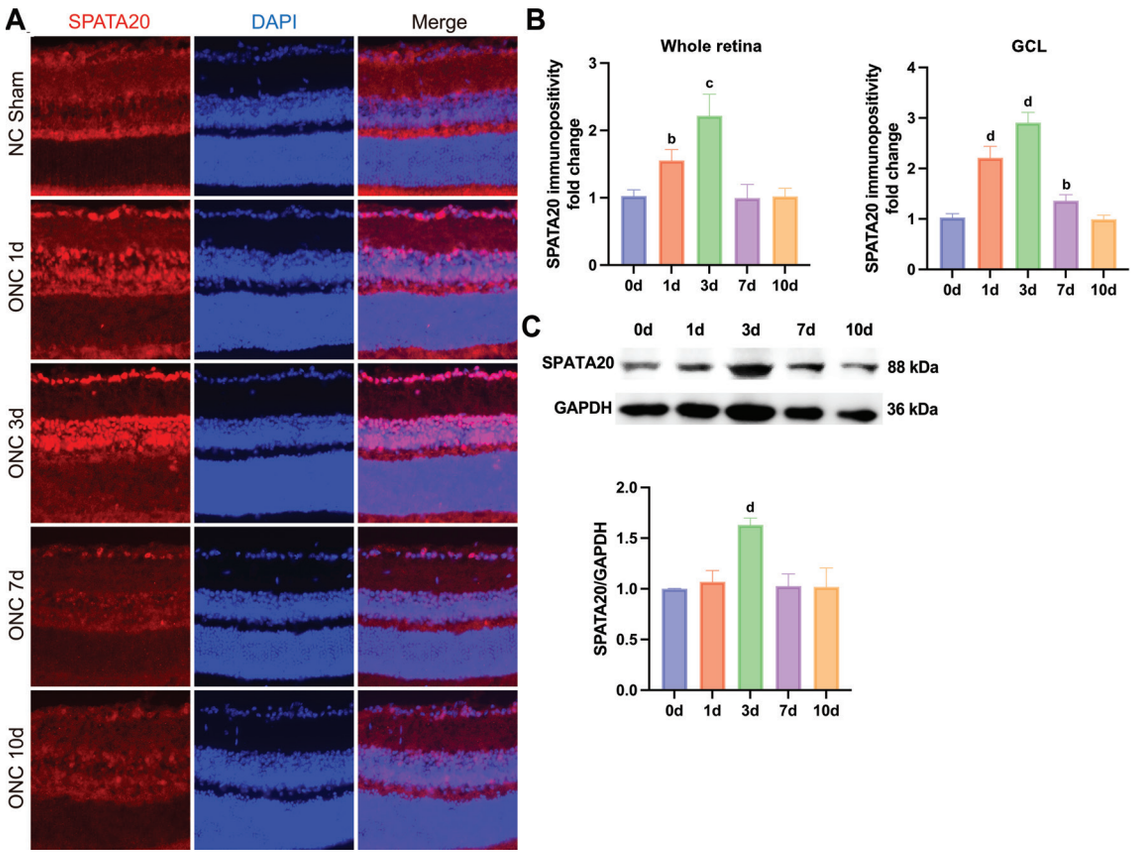

Figure 6 Expression of SPATA20 in glaucomatous mice model A: Immunofluorescence of retinal sections; B: Statistical analysis of fluorescence intensity in the whole retina and the ganglion cell layer; C: Protein expression changes of SPATA20 at different time points in the glaucomatous model, which was normalized to GAPDH. Data are representative of immunofluorescence and Western blot analyses from *n*=6 mice per group. Statistical significance was determined by unpaired Student's *t*-test, comparing each group to the Sham group. ^{b}P<0.01, ^{c}P<0.001, ^{d}P<0.0001. Data are presented as mean±SD. Scale bar=50 μm. DAPI: 4',6-diamidino-2-phenylindole; ONC: Optic nerve crush; NC: Normal control; GCL: Ganglion cell layer; GAPDH: Glyceraldehyde-3-phosphate dehydrogenase; SD: Standard deviation.

DISCUSSION

Given the established contribution of mitochondrial dysfunction to glaucoma, therapeutic strategies targeting mitochondrial genes may provide new avenues to understand and intervene in this neurodegenerative disease[19-20]. Using SMR-based integrative analyses, our study prioritized 18 candidate genes significantly associated with POAG and related traits. Notably, only 4 genes (*DMPK*, *FAM162A*, *PITRM1*, and *SPATA20*) showed directionally consistent effects across methylation, and expression levels, suggesting potential locus- and tissue-specific regulatory architectures.

Among the prioritized genes, *SPATA20* emerged as the top candidate because it was the only gene supported at all three omics levels and showed consistent negative associations with mRNFL thickness at methylation, expression, and protein levels. *SPATA20* is a spermatogenesis-associated gene with an annotated mitochondrial localization. Available evidence from reproductive biology suggests that it participates in sperm structural formation and may be linked to the maintenance of mitochondrial function and energy metabolism[21]. In a Drosophila MYOC transgenic model, the human SPATA20 ortholog (CG8613) was consistently upregulated in eye tissue, accompanying elevated IOP-like changes and progressive visual decline, implying a potential ocular relevance[22]. In our SMR results, *SPATA20* emerged as a prioritized candidate gene for mRNFL, with concordant effect directions at the mQTL, eQTL, and pQTL levels. We further found that SPATA20 is expressed in the GCL of mouse retina, which aligns with its significant association with mRNFL in the SMR analysis. Its transient upregulation in glaucomatous models further implicates it in the RGC-related pathogenesis, yet the potential mechanisms warrant further investigation. Together, the convergent three-omics support plus experimental signal in an optic neuropathy model place *SPATA20* at the top of our prioritization hierarchy as a candidate biomarker and a potential mediator of early RGC-related injury.

Beyond *SPATA20*, several prioritized genes also had glaucoma-relevant support. *NSUN4*, a mitochondrial rRNA methyltransferase essential for mitochondrial ribosome assembly and oxidative phosphorylation[23], has been reported

to support mitochondrial translation and promote RGC survival in rodent glaucoma models, suggesting a neuroprotective role[24]. However, the discordant directions we observed across regulatory layers warrant targeted validation in ocular tissues. *PNPT1*, a mitochondrial RNA-processing factor, has been linked to an optic atrophy family, providing a clinically plausible bridge to optic nerve susceptibility for glaucoma[25], yet its methylation- and expression-based effects were discordant in our data, warranting direct validation in optic nerve tissue. *CYP24A1* participates in vitamin D catabolism in eyes[26-27]. Ocular studies support local vitamin D metabolism and epidemiologic study suggests an inverse relationship between serum 25(OH)D and elevated IOP, which may be related to vitamin D inhibitory effect on trabecular meshwork fibrosis[28-29]. Our findings showed opposite directions between methylation and expression, underscoring the need for eye-specific functional studies. *DMPK* variants have been reported in patients with RNFL defects and increased cup-to-disc ratio without elevated IOP[30], and *DMPK* has also been implicated in other ocular phenotypes, such as early-onset cataract and polypoidal choroidal vasculopathy[30-31]. In our integrative results, *DMPK* showed a consistent protective association with POAG at methylation and transcriptional levels, supporting its candidacy among glaucoma-relevant targets.

Five genes identified in our analysis have been implicated in retinopathy outside glaucoma. *ALAS1*, encoding mitochondrial rate-limiting enzyme in heme biosynthesis, has been shown to be upregulated in retinal degeneration models with proposed mitochondrial protection[32], while *FAM162A* and *GSTZ1* have been associated with age-related macular degeneration[33-34]. *NME3* and *MRPS10* have been implicated in diabetic retinopathy[35-36]. These genes may participate in shared mitochondrial stress pathways across retinal diseases, but their glaucoma-specific relevance remains to be clarified.

Furthermore, 4 genes have been reported to be associated with central nervous system (CNS) disorders. PITRM1 is a mitochondrial matrix peptidase that maintains mitochondrial proteostasis. Impaired PITRM1 can promote amyloid-beta accumulation and neurodegenerative phenotypes[37]. Given proposed overlaps between amyloid-beta biology and glaucoma pathogenesis[38], PITRM1 may represent a molecular link between glaucoma and broader neurodegenerative processes. *VARS2* pathogenic variants underlie combined oxidative phosphorylation deficiency with prominent neurological manifestations[39], underscoring its role in mitochondrial translation and CNS vulnerability. CHCHD4 haploinsufficiency reduces neuronal death in neonatal hypoxia-ischemia models[40], indicating involvement in mitochondrial protein import and injury response. AKAP10, as part of the A-kinase anchoring protein family[41], implicates PKA/G-protein signaling localization that is relevant to neuronal signal transduction, although direct clinical CNS disease associations are not yet established.

In contrast, *DCXR*, *LAP3*, *PDF*, and *CHCHD6* have limited literature linking them to ocular disease or neurodegeneration disorders, although their roles in core metabolic or mitochondrial pathways suggest plausible avenues for future investigation.

Our study has both overlap and clear differences with recent work in this area. Like Jia *et al*[42], we used large scale genetic data to identify glaucoma related candidate signals, but their study focused on plasma proteins and therapeutic target prioritization, whereas ours focused on mitochondrial related molecular traits and included functional validation of SPATA20. Almarzouki[43] identified candidate genes linking glaucoma and high IOP mainly through expression profiling and network analysis, while our study provides genetics based support for candidate signals and adds a different layer of evidence for the molecular basis of glaucoma.

This study has several strengths. First, we combined SMR, HEIDI, and colocalization to strengthen causal inference from summary data. Second, the use of large GWAS datasets improved statistical power. Third, the cross-omic integration provided an evidence hierarchy, enabling prioritization of biologically coherent candidates and identify the most prominently gene *SPATA20*, the unique three-omics-supported target for glaucoma. Finally, the ONC model provided experimental support linking *SPATA20* to glaucomatous neuropathy.

Several limitations should be noted. The limited number of IVs for pQTLs may weaken causal inference for protein targets. The absence of independent datasets for glaucoma-related traits precluded external replication. Additionally, the analyses were restricted to European ancestry, which may limit generalizability and requires validation in other populations.

Our study explored the potential causal relationships of mitochondrial-related gene methylation, expression, and protein abundance with POAG and its related traits, highlighting the significance of several mitochondrial-related genes and their regulatory mechanisms in the pathogenesis of POAG. SPATA20 was the strongest integrative target with convergent genetic and experimental support. These findings not only deepen our understanding of the underlying pathological changes but also offer insight for future pharmacological interventions.

ACKNOWLEDGEMENTS

Authors' Contributions: Conceptualization, investigation, and formal analysis: Luo JY, Ouyang ZK; Methodology: Ge L, Yu ST; Writing-original draft: Luo JY, Yu ST.

Data Availability Statement: Publicly available datasets were

analyzed in this study. Summary statistics are available in the OpenGWAS database (https://gwas.mrcieu.ac.uk/): POAG: ebi-a-GCST90011766; IOP: ebi-a-GCST004074; mRNFL: ebi-a-GCST90014266; mGCIPL: ebi-a-GCST90014267. The supplementary data of this article can be requested from the corresponding author upon reasonable request.

AI-Generated Content Disclosure: Not applicable.

Foundations: Supported by Guangdong Basic and Applied Basic Research Foundation (No.2025A1515010702); Medical Scientific Research Foundation of Guangdong Province of China (No.B2026065).

Conflicts of Interest: Ouyang ZK, None; **Ge L,** None; **Yu ST,** None; **Luo JY,** None.

REFERENCES

1 Beard E, El-Bushra S, Kader Z, *et al*. From regeneration failure to functional restoration: unlocking the neuronal-intrinsic regenerative capacity as a therapeutic frontier for optic neuropathy and glaucoma. *CNS Neurosci Ther* 2026;32(2):e70800.

2 Sun HT, Li B, Gu Y, *et al*. Imbalanced mitochondrial homeostasis in ocular diseases: unique pathogenesis and targeted therapy. *Exp Eye Res* 2025;260:110632.

3 He Y, Leung KW, Zhuo YH, *et al*. Pro370Leu mutant myocilin impairs mitochondrial functions in human trabecular meshwork cells. *Mol Vis* 2009;15:815-825.

4 Milla E, Laguna J, Alforja MS, *et al*. Next-generation sequencing-based gene panel tests for the detection of rare variants and hypomorphic alleles associated with primary open-angle glaucoma. *PLoS One* 2024;19(1):e0282133.

5 Wang SJ, Xiao R, Lu YF, *et al*. Inhibiting NLRP3 inflammasome activation to alleviate retinal inflammation and protect the optic nerve of OPTN(E50K)mice. *Inflammation* 2025;48(4):2105-2121.

6 Liu YF, Luo XY, Zhao ZC, *et al*. Association between optic atrophy 1 polymorphisms and primary open angle glaucoma risk: Based on a meta-analysis. *Eur J Ophthalmol* 2024;34(3):708-718.

7 Smith GR, Zhao BQ, Lindholm ME, *et al*. Multi-omic identification of key transcriptional regulatory programs during endurance exercise training in rats. *Nat Commun* 2026;17(1):4286.

8 Hysi PG, Hardcastle AJ, Davidson AE, *et al*. Influence of inflammatory and metabolic factors on keratoconus risk: a causal inference analysis. *Eye (Lond)* 2026;40(6):842-847.

9 Gharahkhani P, Jorgenson E, Hysi P, *et al*. Genome-wide meta-analysis identifies 127 open-angle glaucoma loci with consistent effect across ancestries. *Nat Commun* 2021;12(1):1258.

10 Zhou W, Zhao ZC, Nielsen JB, *et al*. Scalable generalized linear mixed model for region-based association tests in large biobanks and cohorts. *Nat Genet* 2020;52(6):634-639.

11 McRae AF, Marioni RE, Shah S, *et al*. Identification of 55,000 replicated DNA methylation QTL. *Sci Rep* 2018;8(1):17605.

12 Rath S, Sharma R, Gupta R, *et al*. MitoCarta3.0: an updated mitochondrial proteome now with sub-organelle localization and pathway annotations. *Nucleic Acids Res* 2021;49(D1):D1541-D1547.

13 Võsa U, Claringbould A, Westra HJ, *et al*. Large-scale *cis*- and trans-eQTL analyses identify thousands of genetic loci and polygenic scores that regulate blood gene expression. *Nat Genet* 2021;53(9):1300-1310.

14 Ferkingstad E, Sulem P, Atlason BA, *et al*. Large-scale integration of the plasma proteome with genetics and disease. *Nat Genet* 2021;53(12):1712-1721.

15 Springelkamp H, Iglesias AI, Mishra A, *et al*. New insights into the genetics of primary open-angle glaucoma based on meta-analyses of intraocular pressure and optic disc characteristics. *Hum Mol Genet* 2017;26(2):438-453.

16 Currant H, Hysi P, Fitzgerald TW, *et al*. Genetic variation affects morphological retinal phenotypes extracted from UK Biobank optical coherence tomography images. *PLoS Genet* 2021;17(5):e1009497.

17 Adhikari N, Lunetta KL, Gagnon DR, *et al*. Bayesian Mendelian randomization methods for index trait bias correction in subsequent trait genome-wide association studies. *HGG Adv* 2026;7(3):100592.

18 Luo JY, Lian Q, Zhu DL, *et al*. PLSCR1 promotes apoptosis and clearance of retinal ganglion cells in glaucoma pathogenesis. *Genes Dis* 2023;10(4):1564-1581.

19 Ju WK, Perkins GA, Kim KY, *et al*. Glaucomatous optic neuropathy: Mitochondrial dynamics, dysfunction and protection in retinal ganglion cells. *Prog Retin Eye Res* 2023;95:101136.

20 Yang TH, Kang EY, Lin PH, *et al*. Mitochondria in retinal ganglion cells: unraveling the metabolic nexus and oxidative stress. *Int J Mol Sci* 2024;25(16):8626.

21 Liu M, Ru YF, Gu YH, *et al*. Disruption of Ssp411 causes impaired sperm head formation and male sterility in mice. *Biochim Biophys Acta Gen Subj* 2018;1862(3):660-668.

22 Carbone MA, Ayroles JF, Yamamoto A, *et al*. Overexpression of myocilin in the drosophila eye activates the unfolded protein response: implications for glaucoma. *PLoS One* 2009;4(1):e4216.

23 Ren BC, He KN, Wei N, *et al*. Nanoparticle-delivered siRNA targeting NSUN4 relieves systemic lupus erythematosus through declining mitophagy-mediated $CD8^+$T cell exhaustion. *MedComm (2020)* 2025;6(8):e70311.

24 Li YH, Li D, Geng C, *et al*. The RNA m5C methylase NSUN4 protects retinal ganglion cells by regulating m5C methylation in the Hedgehog signaling pathway. *PREPRINT (Version 1) available at Research Square* 2024. https://doi.org/10.21203/rs.3.rs-4687125/v1.

25 Kuht HJ, Thomas KA, Hisaund M, *et al*. Ocular manifestations of PNPT1-related neuropathy. *J Neuro Ophthalmol* 2021;41(3):e293-e296.

26 Rullo J, Pennimpede T, Mehraban Far P, *et al*. Intraocular calcidiol: Uncovering a role for vitamin D in the eye. *J Steroid Biochem Mol Biol* 2020;197:105536.

27 Markiewicz A, Brożyna AA, Podgórska E, *et al*. Vitamin D receptors (VDR), hydroxylases CYP27B1 and CYP24A1 and retinoid-related orphan receptors (ROR) level in human uveal tract and ocular melanoma with different melanization levels. *Sci Rep* 2019;9(1):9142.

28 Lee JH, Kwon YJ, Lee HS, *et al*. Inverse relationship between serum 25-hydroxyvitamin D and elevated intraocular pressure. *Nutrients* 2023;15(2):423.

29 Morelli-Batters A, Lamont HC, Elghobashy M, *et al*. The role of Vitamin D3 in ocular fibrosis and its therapeutic potential for the glaucomatous trabecular meshwork. *Front Ophthalmol (Lausanne)* 2022;2:897118.

30 Hwang H, Kang MJ, Yim H. Two cases of myotonic dystrophy manifesting various ophthalmic findings with genetic evaluation. *Indian J Ophthalmol* 2016;64(7):535.

31 Iida Y, Hayashi T, Tokuhisa T, *et al*. Polypoidal choroidal vasculopathy in a patient with DMPK-associated myotonic dystrophy. *Doc Ophthalmol* 2022;144(3):217-226.

32 Panagis L, Zhao XJ, Ge YC, *et al*. Retinal gene expression changes related to IOP exposure and axonal loss in DBA/2J mice. *Invest Ophthalmol Vis Sci* 2011;52(11):7807-7816.

33 Hall JC, Krishna Sudhakar K, Daniszewski M, *et al*. Patient induced pluripotent stem cells identify specificities of a reticular pseudodrusen phenotype in age-related macular degeneration. *Genome Med* 2026;18(1):54.

34 Othman H, Saadat I, Farvardin-Jahromi M, *et al*. Susceptibility to exudative age-related macular degeneration and three genetic polymorphisms of glutathione S-transferase Z1 (GSTZ1). *Eur J Ophthalmol* 2012;22(3):431-435.

35 Liu C, Chen GJ, Bentley AR, *et al*. Genome-wide association study for proliferative diabetic retinopathy in Africans. *NPJ Genom Med* 2019;4:20.

36 Shen YQ. High expression of Mrps10 in diabetic retinopathy: a bioinformatics analysis based on public transcriptomic data. *Medicine (Baltimore)* 2025;104(35):e44179.

37 Brunetti D, Torsvik J, Dallabona C, *et al*. Defective PITRM1 mitochondrial peptidase is associated with Aβ amyloidotic neurodegeneration. *EMBO Mol Med* 2016;8(3):176-190.

38 Yoshida Y, Michihata N, Tanito M, *et al*. Association between open angle glaucoma and early onset Alzheimer's disease. *J Alzheimers Dis* 2026;110(1_suppl):S30-S37.

39 Bruni F, Di Meo I, Bellacchio E, *et al*. Clinical, biochemical, and genetic features associated with *VARS2*-related mitochondrial disease. *Hum Mutat* 2018;39(4):563-578.

40 Sun YY, Li T, Xie CC, *et al*. Haploinsufficiency in the mitochondrial protein CHCHD4 reduces brain injury in a mouse model of neonatal hypoxia-ischemia. *Cell Death Dis* 2017;8(5):e2781.

41 Sharma K, Saini N, Hasija Y. Identifying the mitochondrial metabolism network by integration of machine learning and explainable artificial intelligence in skeletal muscle in type 2 diabetes. *Mitochondrion* 2024;74:101821.

42 Jia DD, Xiao QA, Song SY, *et al*. Identification of novel drug targets for primary open angle glaucoma and its potential side-effects by human plasma proteome. *Int J Ophthalmol* 2025;18(8):1470-1477.

43 Almarzouki N. NMI, POLR3G and APIP are the key molecules connecting glaucoma with high intraocular pressure: a clue for early diagnostic biomarker candidates. *Int J Ophthalmol* 2024;17(11):1987-1994.